

Counter-flow induced clustering: exact results

Amit Kumar Chatterjee*

Yukawa Institute for Theoretical Physics, Kyoto University

Hisao Hayakawa†

Yukawa Institute for Theoretical Physics, Kyoto University and
Center for Gravitational Physics and Quantum Information,
Yukawa Institute for Theoretical Physics, Kyoto University

We analyze the cluster formation in a non-ergodic stochastic system as a result of counter-flow, with the aid of an exactly solvable model. To illustrate the clustering, a two species asymmetric simple exclusion process with impurities on a periodic lattice, is considered. Exact analytical results show two distinct phases, *free flowing phase* (non-monotonic density and finite current of the non-conserved species) and *clustering phase* (constant density and vanishing current of the same). We define a rearrangement parameter capturing the effect of non-ergodicity on clustering.

Introduction.- Clustering of non-attractive elements is an intriguing phenomenon occurring in diverse areas of science and society. It appears in various fields such as granular materials [1–3], vehicular and pedestrian traffic flows [4–7], active matter [8, 9], biology [10, 11] etc. At the heart of the clustering phenomena lies a transition between free flowing phase and jammed phase where motion becomes highly restrictive, as some suitable system parameter is tuned. The tuning parameter for granular material is packing fraction, for traffic flow it is car or pedestrian density and self-propulsion force in case of dense active matter. In fact, a jamming phase diagram has been proposed keeping in mind the generality of such transitions [1] and there are experiments conducted on colloidal particles supporting the concept of this generic phase diagram [12]. The control of clustering is important in daily life. Indeed, understanding the formation of jamming and finding ways to transit to unjammed state, has immense importance in traffic science. The other applications include occurrence of cellular jamming transitions in cancer [10, 11]. Analysis of clustering, as a phase transition in interacting many body systems, constitutes an interesting topic from the physics point of view. Thus, it seems natural to investigate the clustering phenomena through the lens of statistical mechanics.

It is possible to observe phase transitions even in one dimension, for long range interacting systems in equilibrium [13–18], and for non-equilibrium systems remarkably with short range interactions [19–28]. In context of short range interactions, these one dimensional non-equilibrium models with simplified local dynamics, are amenable to exact analytical calculations and thereby provide much insights to the microscopic origins of the phase transitions [29, 30]. In context of cluster formations in disordered systems, Bose-Einstein condensates have been studied in multi-species asymmetric simple exclusion processes [31, 32], utilizing matrix product ansatz

[33] and zero range process [34, 35]. Spontaneous symmetry breaking in a model with two oppositely moving particles with exchange interaction, has been discussed with periodic boundaries [36, 37] and open boundaries [38]. However, later it has been proved that the spatial condensation of particles under periodic boundary condition [37], is not associated with a phase transition in the grand canonical ensemble [39, 40]. Jamming in more realistic traffic models like bus route models, has been considered [41, 42] and its connection to Nagel-Schreckenberg model of traffic flow, has been explored in details [43]. There are various other interesting studies of one dimensional traffic flows under periodic boundary conditions [4–7, 44–47]. Notably, once a formed cluster is stable and moves in one-direction, it is similar to the time-crystal [48–52]. To avoid such clustering, model with bypassing defects through long range hopping, has been analyzed [53]. However, exact analytical results showing clustering phenomenon has been considerably few.

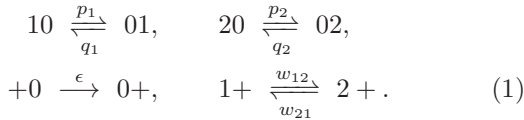
In this work, we discuss exact results for the cluster formation on a one dimensional periodic lattice, when counter-flow is present in the system. Two additional features of *non-ergodicity* and *non-conserving* dynamics, are taken into account. As a model, we consider the two species asymmetric simple exclusion process with impurity activated flips (2-ASEP-IAF) [54]. We provide exact analytical expressions for one-point (average species densities), two-point (drift current) and n -point functions (correlation between consecutive vacancies). All of them indicate the existence of two-different phases: the *free flowing phase* and the *clustering phase*. Particularly, the n -point correlation function increases with increasing n in the counter-flow phase, directly pointing towards the clustering of vacancies and consequently clustering of particles in the model. The model considered here, being non-ergodic, acts as a natural playground to address the role of initial configurations on the cluster formation. Surprisingly, depending on the initial arrangements of the particles, we see considerable shift in the onset of cluster formation in the counter-flow phase.

Model.- We consider two different species (1 and 2)

* ak.chatterjee@yukawa.kyoto-u.ac.jp

† hisao@yukawa.kyoto-u.ac.jp

along with impurities (+) and vacancies (0) on a one-dimensional periodic lattice. Both species can hop to right (with rates p_1 and p_2) or to left (with rates q_1 and q_2) nearest neighbor if vacant, whereas the impurity can hop only towards right (with rate ϵ). Alongside the hopping dynamics, species 1 and 2 can transform into each other (with rates w_{12} and w_{21}), such flipping being activated only in presence of impurity. The microscopic dynamics can be represented as



We would vary q_1 as our tuning parameter, keeping all other rates fixed. We choose $p_2 > q_2$ and $\epsilon > 0$. Subsequently, if $q_1 < p_1$, each species and impurity have net bias along the same direction, keeping the system in *natural flow*. On the other hand, when $q_1 > p_1$, species 1 has net bias in the direction opposite to the net bias of species 2 and impurities, thereby species 1 opposes the motion of other components and creates a *counter-flow* situation. Since the tuning parameter q_1 can control the flow situation in the system, we denote it as the *counter-flow parameter*. The densities $\rho_0 = N_0/L$ and $\rho_+ = N_+/L$, of vacancies and impurities, respectively, are conserved quantities.

Steady state.- The steady state of this model can be obtained as a matrix product state and probability $P(\{s_i\})$ of any configuration $\{s_i\}$ can be expressed as $P(\{s_i\}) \propto \text{Tr} \left[\prod_{i=1}^L X_i \right]$ [54]. Here X_i is a matrix representing the constituent s_i at lattice site i , $X_i = E\delta_{s_i,0} + A\delta_{s_i,+} + D_1\delta_{s_i,1} + D_2\delta_{s_i,2}$. The matrices D_1, D_2, A, E ; representing species 1, species 2, impurity and vacancy, respectively; have infinite dimensional representations. See Ref. [54] for details. However, the calculations of the partition function and observables strongly depend on the choice of initial configurations, owing to the non-ergodicity resulting from the microscopic dynamics.

Initial configuration.- In spite of the presence of flip-dynamics, the microscopic dynamics in Eq. (1) preserves certain orderings of the different species and impurities from initial configuration. It implies that the system can access only a subspace of the whole configuration space, starting from a particular initial configuration. For our purpose, we consider the following initial configuration (represented by corresponding matrices),

$$D_2A \dots D_2A D_1A \dots D_1A D_1 \dots D_1 E \dots E. \quad (2)$$

The dots in $\mathcal{Y} \dots \mathcal{Y}$ represent an uninterrupted sequence of the unit \mathcal{Y} . In Eq. (2), we have four such sequences with $\mathcal{Y} = D_2A, D_1A, D_1$ and E . Note that, there are two types of species 1 particles in Eq. (2). One type is those which can flip, belongs to the sequence $\mathcal{Y} = D_1A$, while the others are non-flipping species 1 particles belonging to the sequence $\mathcal{Y} = D_1$. The density of such non-flipping species 1 particles is denoted by $\bar{\rho} = \bar{N}/L$.

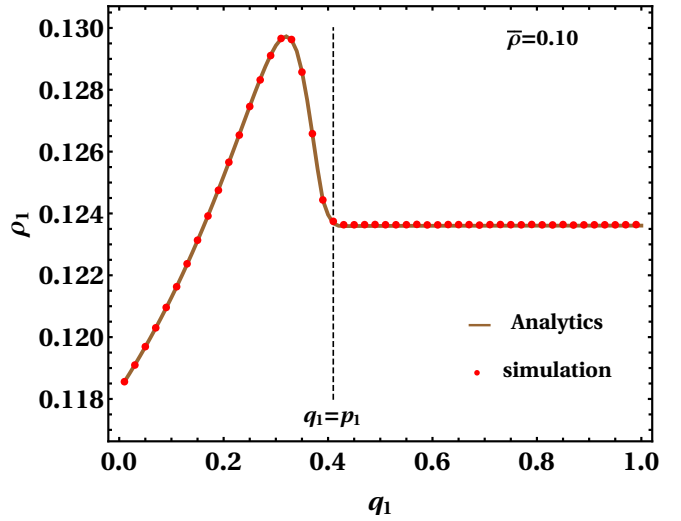


FIG. 1. The figure shows the behavior of the average species density as a function of the counter-flow parameter, obtained from analytical result (brown solid line) and Monte Carlo simulation (red dots). Two different phases are apparent, separated by the transition point $q_1 = p_1$. For $q_1 < p_1$, the density exhibits non-monotonicity whereas for $q_1 > p_1$ the density remains constant. The parameters used are $L = 10^3, p_1 = 0.4, p_2 = 1.0, q_2 = 0.5, \epsilon = 0.1, w_{12} = 1.0, w_{21} = 0.1, \rho_+ = 0.25, \rho_0 = 0.4$.

Two phases: analytical results.- For the initial configuration Eq. (2), we can calculate analytically the partition function and observables of interest using the explicit representations of the matrices. For detailed calculations, see Ref. [55]. It is fascinating that even the simplest one-point function, namely the average species density, indicates the existence of two different phases. In Fig. 1, we present the corresponding analytical results for average density ρ_1 of species 1, agreeing with the Monte Carlo simulation results, as a function of the counter-flow parameter q_1 . It is observed that the density exhibits a non-monotonic behavior in the parameter region $q_1 < p_1$, whereas it remains constant for $q_1 > p_1$. As one increases q_1 starting from zero, the hopping of species 1 particles to left, becomes increasingly likely. This means lesser chances for species 1 particles to have impurities as their right nearest neighbors. Consequently, the flipping of species 1 to 2 decreases with increasing q_1 , and therefore ρ_1 increases. This is followed by an abrupt fall near $q_1 \lesssim p_1$. For $q_1 > p_1$, the density remains constant indicating that the drift process no longer can affect ρ_1 , meaning the species 1 particles cannot access vacancies due to possible clustering. The point $q_1 = p_1$ demarcating two different phases, is regarded as the transition point. We find the exact formulae for the average species densities to be

$$\rho_1 = \bar{\rho} + \left(\rho_+ - \frac{1}{L} \right) \frac{\frac{w_{21}}{1 - \frac{z_0}{p_1} S_0}}{\left[\frac{w_{21}}{1 - \frac{z_0}{p_1} S_0} + \frac{w_{12}}{1 - \frac{z_0}{p_2} (1 + \frac{q_2}{p_1} S_{-1})} \right]}$$

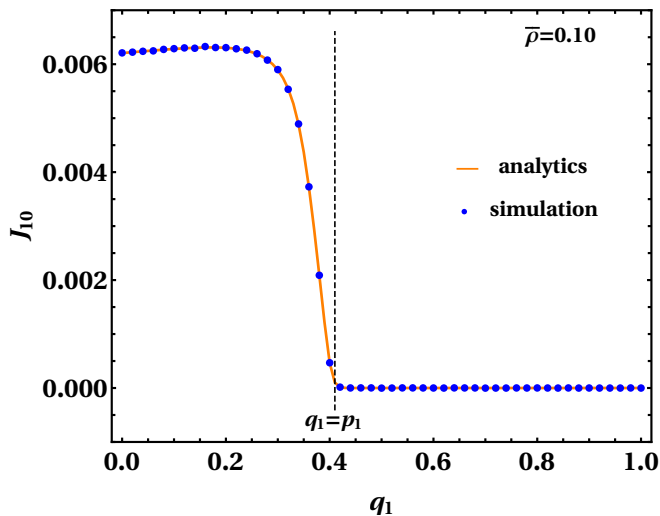


FIG. 2. The figure demonstrates two different phases manifested by the drift current, obtained from analytical result (orange solid line) and Monte Carlo simulation (blue dots). In the parameter regime $q_1 < p_1$, the current is finite whereas it falls abruptly to vanishingly small values at $q_1 = p_1$ and remains so for $q_1 > p_1$. The parameters used are $L = 10^3$, $p_1 = 0.4$, $p_2 = 1.0$, $q_2 = 0.5$, $\epsilon = 0.1$, $w_{12} = 1.0$, $w_{21} = 0.1$, $\rho_+ = 0.25$, $\rho_0 = 0.4$.

$$\rho_2 = \bar{\rho} + \rho_+ - \rho_1, \quad (3)$$

$$+ \frac{1}{L} \left[\frac{\frac{w_{21}}{1 - \frac{z_0}{p_1} S_N}}{\frac{w_{21}}{1 - \frac{z_0}{p_1} S_N} + \frac{w_{12}}{1 - \frac{z_0}{p_2} (1 + \frac{q_2}{p_1} S_{N-1})}} \right],$$

where $S_k = \sum_{j=0}^k \left(\frac{q_1}{p_1}\right)^j + \left(\frac{q_1}{p_1}\right)^k \frac{q_1}{\epsilon}$ and the fugacity z_0 can be obtained by solving the density-fugacity relation

$$\frac{z_0}{L} \frac{d}{dz_0} \ln(Q) = \rho_0, \quad (4)$$

with Q being the partition function [55].

The drift currents for the non-conserved species and the impurity are given by

$$J_{\alpha 0} = z_0 \rho_{\alpha}, \quad \alpha = 1, 2, +. \quad (5)$$

The average steady state densities of the non-conserved species are provided in Eq. (3) whereas the impurity density ρ_+ is a conserved quantity, the fugacity obeys Eq. (4). We study the average drift current J_{10} for species 1 in Fig. 2 to analyze the transport or flow of the constituents in the two different phases apparent from Fig. 1. Interestingly, the current exhibits a sharp fall near the transition point $q_1 = p_1$, and it remains almost zero (i.e. vanishingly small values) in the phase ($q_1 > p_1$) where the average density remains constant. Also, the species 2 and impurity have same characteristics of current. A natural subsequent question is, what makes the system to have non-changing density and vanishing current in the parameter regime $q_1 > p_1$. The vanishing current implies

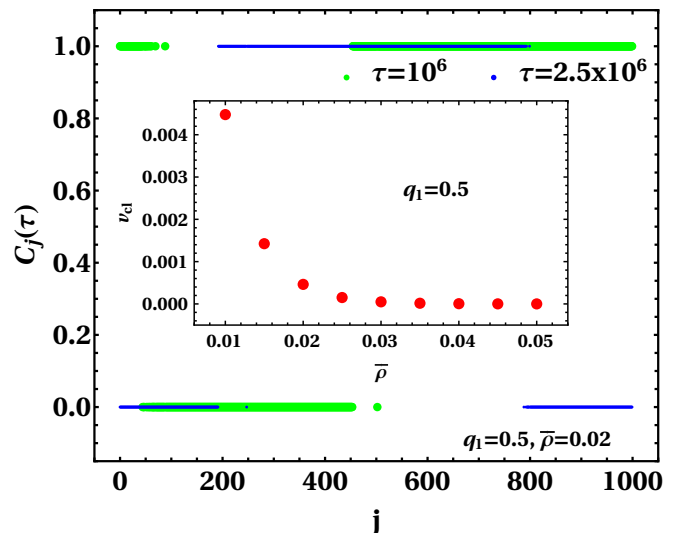


FIG. 3. The figure shows Monte Carlo simulation results for the formation of two macroscopic clusters of particles and vacancies for $q_1 > p_1$. The cluster of particles shifts towards right with small velocity. This slow drift, characterized by the cluster velocity v_{c1} , is presented in the inset with the variation of $\bar{\rho}$. The parameters used are $L = 10^3$, $p_1 = 0.4$, $p_2 = 1.0$, $q_2 = 0.5$, $\epsilon = 0.1$, $w_{12} = 1.0$, $w_{21} = 0.1$, $\rho_+ = 0.29$ and $\rho_0 = 1 - 2\rho_+ - \bar{\rho}$.

that the motions of the particles have become highly restrictive and the drift almost ceases to exist, indicating possible clustering.

Cluster formation.- To understand the microscopic origin of such restrictive drift, we focus on the following quantity

$$C_j(\tau) = \begin{cases} 1 & \text{if } s_j = 1 \text{ or } s_j = 2 \text{ or } s_j = + \\ 0 & \text{if } s_j = 0. \end{cases} \quad (6)$$

In the steady state, $C_j(\tau)$ simply measures if there is a particle at lattice site j or it is vacant in the configuration at time τ . From the results of Monte Carlo simulation (see Fig. 3), we observe that two macroscopic clusters are formed in the system at any time τ , one consisting of all the particles (both species and impurities) and the other accumulates all the vacancies. Further, we notice that this cluster of particles shifts towards right with negligible velocity and this shift is visible only for large enough $\Delta\tau$ between two observations. This slow shift of the cluster is similar to time crystals [48–52]. Note that the slow shift in our model is caused by the unidirectional motion of impurities, and thus the emergence of this slow shift is not contradictory with the no-go theorem of time-crystals [50]. The eventual shifts of the clusters imply that the density profile would be homogeneous when the ensemble average is performed over sufficiently large number of samples. This in turn means that the existence of two different phases (Figs. 1 and 2) can not be seen from the density profiles, rather the clustering becomes visible by tracking individual configurations $C_j(\tau)$. To get an estimate of the cluster velocity v_{c1} we

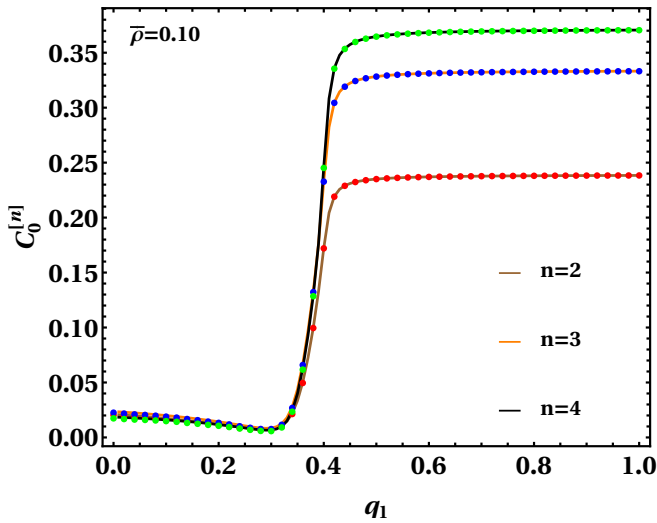


FIG. 4. The figure shows abrupt change in the n -point correlation between consecutive vacancies near the transition point $q_1 = p_1$. For $q_1 > p_1$, the growth of the correlation with increasing n implies the tendency of vacancies to form larger cluster. Solid lines and dots correspond to analytical calculation and Monte Carlo simulation results respectively. The parameters used are $L = 10^3$, $p_1 = 0.4$, $p_2 = 1.0$, $q_2 = 0.5$, $\epsilon = 0.1$, $w_{12} = 1.0$, $w_{21} = 0.1$, $\rho_+ = 0.25$, $\rho_0 = 0.4$.

compute the displacement of the impurity sitting at the left end of the cluster, the corresponding result as a function of the density $\bar{\rho}$ is shown in the inset of Fig. 3. We observe that, with increasing $\bar{\rho}$, the cumulative effect of non-flipping species 1 particles (prone towards left hopping) increases and thereby the cluster velocity (towards right) decreases.

The analysis of Figs. 1 and 2 supported by Fig. 3, lead us to name the two phases as *free flowing phase* and *clustering phase*. It is important to note that the transition point occurs at $q_1 = p_1$ meaning that sufficiently small counter-flow is enough to impose clustering in the system.

An illuminating way to analytically show the formation of clusters, is to calculate the n -point correlation between consecutive vacancies (it is more helpful than calculating correlations between particles, because we have mixture of different species and impurities inside the particle cluster). We have obtained the expression for n -point correlation $C_0^{[n]} = \langle 00 \dots 0 \rangle - \langle 0 \rangle^n$, between n consecutive vacancies, in a recursive manner, see Ref. [55] for details. The superscript $[n]$ represents the length of the uninterrupted sequence of consecutive vacancies (0, in subscript). We present the variation of $C_0^{[n]}$ with the counter-flow parameter for different values of n in Fig. 4. Interestingly, the correlations between consecutive vacancies increase considerably with increasing n for $q_1 > p_1$. Clearly, more number of vacancies prefer to stick together in the parameter regime $q_1 > p_1$. This is a direct evidence of macroscopic cluster formation of vacancies in the clustering phase.

Non-ergodicity and clustering.- Finally, we would like

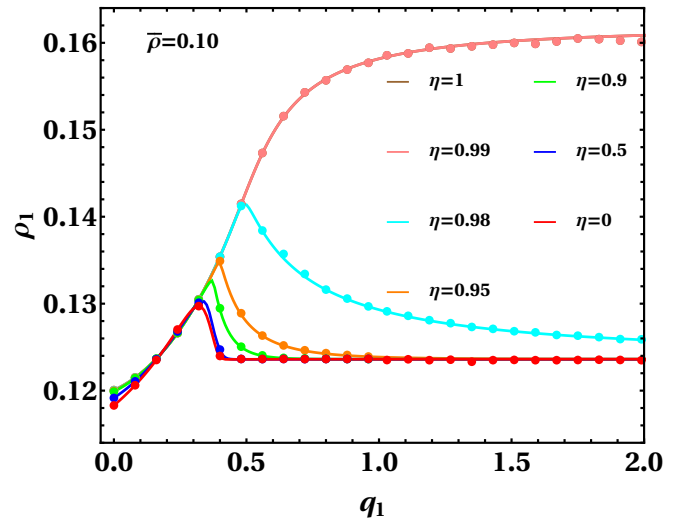


FIG. 5. The figure demonstrates the effect of rearrangement parameter η (characterizing non-ergodicity) on the clustering phase. As η decreases, the distinction between the free flowing phase and clustering phase becomes more and more abrupt. Particularly, the density remains monotonic for large $\eta \approx 1$, whereas it is non-monotonic for small and moderate values of η . Solid lines and dots correspond to analytical calculation and Monte Carlo simulation results respectively. The parameters used are $L = 10^3$, $p_1 = 0.4$, $p_2 = 1.0$, $q_2 = 0.5$, $\epsilon = 0.1$, $w_{12} = 1.0$, $w_{21} = 0.1$, $\rho_+ = 0.25$, $\rho_0 = 0.4$.

to investigate the effect of non-ergodicity on the clustering phenomena. To this end, we consider the following variation of the initial configuration Eq. (2)

$$D_2 A \dots D_2 A \quad D_1 D_1 A \dots D_1 D_1 A \quad D_1 A \dots D_1 A \quad D_1 \dots D_1 \quad E \dots E, \quad (7)$$

where we keep all the input parameters ($p_{1,2}$, ϵ , $w_{12,21}$, ρ_0 , ρ_+ , $\bar{\rho}$) same both for Eqs. (2) and (7). The difference between these two initial configurations lies in the *rearrangement* of the non-flipping species 1 particles. In Eq. (7), we have two types of non-flipping species 1 particles, *isolated* (left D_1 of unit $D_1 D_1 A$, cannot come in contact with another non-flipping D_1), and *non-isolated* (belongs to sequence $D_1 \dots D_1$). For Eq. (2), we have only the non-isolated type. However, the total density of non-flipping D_1 is $\bar{\rho}$, same for both Eq. (2) and Eq. (7). To quantify their difference, we denote the fraction of isolated non-flipping species 1 particles in Eq. (7) as η . Equation (2) corresponds to $\eta = 0$. Since the variation of η simply rearranges the non-flipping D_1 -s in the initial configuration, we denote it as *rearrangement parameter*. Thus η appears as a hallmark of non-ergodicity. We present the behavior of average species density ρ_1 as a function of η in Fig. 5, obtained from analytical calculations [55]. With decreasing η , the distinction between two phases become more evident and the fall of the density to constant value gets sharper. Intriguingly, for small or moderate values of rearrangement parameter, the density is non-monotonic, contrary to its monotonic nature for $\eta \approx 1$.

Discussion.- We have demonstrated the formation of clusters induced by counter-flow in a non-ergodic system. To illustrate this, we have considered two species asymmetric simple exclusion process along with impurities that activate transformation between the two species. This model shows two distinct phases, *free flowing phase* and *clustering phase*, as a function of the counter-flow parameter. Interestingly, simple one point function like average species density indicates the existence of two different phases characterized by non-monotonic density followed by a sudden fall to constant density. The two phases are also evident from the behavior of drift current that becomes vanishingly small in the clustering phase. Remarkably, we provide analytical expressions for species densities, currents as well as n -point correlation between consecutive vacancies. Specifically, the increase in n -point correlation with increasing n directly implies the accumulation of vacancies to form one macroscopic

cluster. The slow drift of the cluster can be observed by tracking individual configurations over long time. The non-ergodicity of the system is characterized through a rearrangement parameter. We believe that our analysis supported by exact analytical results enlightens the understanding of clustering phenomena. The model studied here, having resemblance to multi-lane traffics, naturally points towards analytical understanding of jamming in traffic flows. It would be interesting to study further variations of the local microscopic dynamics considered here, that can produce dynamical ways to get rid of the clustering phase.

Acknowledgements.- This work is partially supported by the Grants-in-Aid for Scientific Research (Grant No. 21H01006). A.K.C. gratefully acknowledges postdoctoral fellowship from the YITP. The numerical calculations have been done on the cluster Yukawa-21 at the YITP.

-
- [1] A. Liu, and S. R. Nagel, *Nature* **396**, 21 (1998), doi:10.1038/23819.
- [2] G. Biroli, *Nature Physics* **3**, 222 (2007), doi:10.1038/nphys580.
- [3] R. P. Behringer, and B. Chakraborty, *Rep. Prog. Phys.* **82**, 012601 (2019), doi:10.1088/1361-6633/aadc3c.
- [4] K. Nagel, and M. Schreckenberg, *J. Phys. I* **2**, 2221 (1992), doi:10.1051/jp1:1992277.
- [5] D. Helbing, *Rev. Mod. Phys.* **73**, 1067 (2001), doi:10.1103/RevModPhys.73.1067.
- [6] T. Nagatani, *Rep. Prog. Phys.* **65**, 1331 (2002), doi:10.1088/0034-4885/65/9/203.
- [7] A. Schadschneider, D. Chowdury and K. Nishinari, *Stochastic transport in complex system: From molecules to vehicles* (Elsevier, Amstrdam, 2011).
- [8] R. Mandal, P. J. Bhuyan, P. Chaudhuri, C. Dasgupta, and M. Rao, *Nat Commun.* **11**, 2581 (2020), doi:10.1038/s41467-020-16130-x.
- [9] J. Yang, R. NI, and J. P. Ciamarra, *Phys. Rev. E* **106**, L012601 (2022), doi:10.1103/PhysRevE.106.L012601.
- [10] M. Sadati, N. T. Quazvini, R. Krishnan, C. Y. Park, and J. J. Fredberg, *Differentiation* **86**, 121 (2013), doi:10.1016/j.diff.2013.02.005.
- [11] L. Oswald, S. Grosser, D M. Smith, and J. A. Käs, *J. Phys. D: Appl. Phys.* **50**, 483001 (2017), doi:10.1088/1361-6463/aa8e83.
- [12] V. Trappe, V. Prasad, L. Cipelletti, P. N. Segre, and D. A. Weitz, *Nature* **411**, 772 (2001), doi:10.1038/35081021.
- [13] M. Antoni, and S. Ruffo, *Phys. Rev. E* **52**, 2361 (1995), doi:10.1103/PhysRevE.52.2361.
- [14] J. Barré, D. Mukamel, and S. Ruffo, *Phys. Rev. Lett.* **87**, 030601, (2001), doi:10.1103/PhysRevLett.87.030601.
- [15] F. Bouchet, and J. Barré, *J. Stat. Phys.* **118**, 1073 (2005), doi:10.1007/s10955-004-2059-0.
- [16] A. Campa, T. Dauxois, and S. Ruffo, *Physics Reports* **480**, 57 (2009), doi:10.1016/j.physrep.2009.07.001.
- [17] Y. Levin, R. Pakter, F. B. Rizzato, T. N. Teles, and F. P. C. Benetti, *Physcs Reports* **535**, 1 (2014), doi:10.1016/j.physrep.2013.10.001.
- [18] I. Latella, A. Perez-Madrid, A. Campa, L. Casetti, and S. Ruffo, *Phys. Rev. Lett.* **114**, 230601 (2015), doi:10.1103/PhysRevLett.114.230601.
- [19] B. Schmittmann and R. K. P. Zia, in *Phase Transitions and Critical Phenomena*, edited by C. Domb and J. Lebowitz (Academic, London, 1994), Vol. 17.
- [20] V. Privman, *Nonequilibrium Statistical Mechanics in One Dimension* (Cambridge University Press, 1997).
- [21] J. Marro and R. Dickman, *Nonequilibrium Phase Transition in Lattice Models* (Cambridge University Press, Cambridge, 1999).
- [22] G.M. Schütz, in C.Domb and J.Lebowitz (eds.) *Phase Transitions and Critical Phenomena*, Vol.19 (Academic, London, 2001).
- [23] M. Henkel, H. Hinrichsen, and S. Lübeck, *Non-Equilibrium Phase Transitions: Volume 1: Absorbing Phase Transitions* (Springer, Netherlands, 2008).
- [24] M. Henkel, and M. Pleimling, *Non-Equilibrium Phase Transitions: Volume 2: Ageing and Dynamical Scaling Far from Equilibrium* (Springer, Netherlands, 2010).
- [25] B. Derrida, S. A. Janowsky, J. L. Lebowitz and E. R. Speer, *J. Stat. Phys.* **73**, 813 (1993), doi:10.1007/BF01052811.
- [26] M. R. Evans, Y. Kafri, H. M. Koduvely, and D. Mukamel, *Phys. Rev. Lett.* **80**, 425 (1998), doi:10.1103/PhysRevLett.80.425.
- [27] R. Lahiri, S. Ramaswamy, *Phys. Rev. Lett.* **79**, 1150 (1997), doi:10.1103/PhysRevLett.79.1150.
- [28] M. R. Evans, Y. Kafri, E. Levine, and D. Mukamel, *J. Phys. A: Math. Gen.* **35**, L433 (2002), doi:10.1088/0305-4470/35/29/101.
- [29] M .R. Evans, *Brazilian Journal of Physics* **30**, 42 (2000), doi:10.1590/S0103-97332000000100005.
- [30] D. Mukamel, [arXiv:cond-mat/0003424](https://arxiv.org/abs/cond-mat/0003424) (2000).
- [31] M. R. Evans, *Europhys. Lett.* **36**, 13 (1996), doi:10.1209/epl/i1996-00180-y.
- [32] J. Krug, and P. A. Ferrari, *J. Phys. A: Math. Gen.* **29**, L465 (1996), doi:10.1088/0305-4470/29/18/004.
- [33] R. A. Blythe, and M. R. Evans, *J. Phys. A: Math. Theor.* **40**, R333 (2007), doi:10.1088/1751-8113/40/46/R01.
- [34] F. Spitzer, *Adv. in Math.* **5**, 246 (1970), doi:

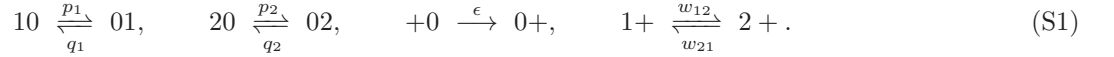
- 10.1016/0001-8708(70)90034-4.
- [35] M. R. Evans, and T. Hanney, *J. Phys. A: Math. Gen.* **38**, R195 (2005), doi:10.1088/0305-4470/38/19/R01.
- [36] H-W Lee, V. Popkov, and D. Kim, *J. Phys. A: Math. Gen.* **30**, 8497 (1997), doi:10.1088/0305-4470/30/24/014.
- [37] P. F. Arndt, T. Heinzl, and V. Rittenberg, *J. Phys. A: Math. Gen.* **31**, L45 (1998), doi:10.1088/0305-4470/31/2/001.
- [38] M. R. Evans, D. P. Foster, C. Godreche, and D. Mukamel, *Phys. Rev. Lett.* **74**, 208 (1995), doi:10.1103/PhysRevLett.74.208.
- [39] N. Rajewsky, T. Sasamoto, and E. R. Speer, *Physica A* **279**, 123 (2000), doi:10.1016/S0378-4371(99)00537-3.
- [40] T. Sasamoto, and D. Zagier, *J. Phys. A: Math. Gen.* **34**, 5033 (2001), doi:10.1088/0305-4470/34/24/302.
- [41] O. J. O. Loan, M. R. Evans, and M. E. Cates, *Phys. Rev. E* **58**, 1404 (1998), doi:10.1103/PhysRevE.58.1404.
- [42] O. J. O. Loan, M. R. Evans, and M. E. Cates, *Europhys. Lett.*, **42**, 137 (1998), doi:10.1209/epl/i1998-00219-7.
- [43] D. Chowdhury, and R. C. Desai, *Eur. Phys. J. B* **15**, 375 (2000), doi:10.1007/s100510051139.
- [44] M. Bando, K. Hasebe, A. Nakayama, A. Shibata, and A. Sugiyama, *Phys. Rev. E* **51**, 1035 (1995), doi:10.1103/PhysRevE.51.1035.
- [45] T. S. Komatsu and S. Sasa, *Phys. Rev. E* **52**, 5574 (1995), doi:10.1103/PhysRevE.52.5574.
- [46] H. Hayakawa and K. Nakanishi, *Phys. Rev. E* **57**, 3839 (1998), doi:10.1103/PhysRevE.57.3839.
- [47] Y. Igarashi, K. Itoh, K. Nakanishi, K. Ogura and K. Yokokawa, *Phys. Rev. Lett.* **83**, 718 (1999), doi:10.1103/PhysRevLett.83.718.
- [48] F. Wilczek, *Phys. Rev. Lett.* **109**, 160401 (2012), doi:10.1103/PhysRevLett.109.160401.
- [49] A. Shapere, and F. Wilczek, *Phys. Rev. Lett.* **109**, 160402 (2012), doi:10.1103/PhysRevLett.109.160402.
- [50] H. Watanabe and M. Oshikawa, *Phys. Rev. Lett.* **114**, 251603 (2015), doi:10.1103/PhysRevLett.114.251603.
- [51] N. Y. Yao, A. C. Potter, I.-D. Potirniche, and A. Vishwanath, *Phys. Rev. Lett.* **118**, 030401 (2017), doi:10.1103/PhysRevLett.118.030401.
- [52] D. W. Else, C. Monroe, C. Nayak, and N. Y. Yao, *Annual Review of Condensed Matter Physics*. **11**, 467 (2020), doi:10.1146/annurev-conmatphys-031119-050658.
- [53] J. Szavits-Nossan, and K. Uzelac, *J. Stat. Mech.* (2011) P05030, doi:10.1088/1742-5468/2011/05/P05030.
- [54] A. K. Chatterjee, and H. Hayakawa, [arXiv:2205.03082](https://arxiv.org/abs/2205.03082) (2022).
- [55] See supplemental material.

SUPPLEMENTAL MATERIAL

This supplemental material explains the details of calculations that are not included in the main text, alongside some further discussions. In Sec. I we explain the exact steady state of the model described by the matrix product ansatz. We elaborate the calculation of the partition functions starting from specific initial configuration in Sec. II. The analytical expressions for average species densities, drift currents and spatial correlations are derived in Sec. III. In Sec. IV, we present the explicit form of the density-fugacity relation and discuss special cases for which exact solution for the fugacity can be obtained. We make some comments regarding the generality of the initial configuration considered in the main text, in Sec. V. In Sec. VI, we compare between our model and the Arndt-Heinzel-Rittenberg (AHR) model [S1] of counter-flow, in context of cluster formation.

I. MATRIX PRODUCT STEADY STATE

The model considered in the main text is a special case of the multi-species asymmetric simple exclusion process with impurity activated flips (μ -ASEP-IAF), studied elaborately in Ref. [S2] using matrix product ansatz. Specifically, we have analyzed the $\mu = 2$ case in the main text, meaning the system consists of two non-conserved species 1 and 2, vacancies (0) and impurities (+). For completeness, we start by mentioning the microscopic dynamics of the 2-ASEP-IAF model,



Here we sketch the main steps to acquire the steady state for the dynamics Eq. (S1) in matrix product form. We make the following ansatz, hypothesizing that the probability of any configuration $\{s_i\}$ ($s_i = 1, 2, 0, +$ denoting the state at site i) can be written as (the trace of) a product of matrices

$$P(\{s_i\}) \propto \text{Tr} \left[\prod_{i=1}^L X_i \right],$$

$$X_i = D_1 \delta_{s_i,1} + D_2 \delta_{s_i,2} + A \delta_{s_i,+} + E \delta_{s_i,0}. \quad (\text{S2})$$

In Eq. (S2), the matrix X_i represents the state s_i of site i and $\delta_{(\cdot),(\cdot)}$ is the Kronecker Delta symbol. The configurations of the system evolve according to the Master equation

$$\frac{d|P\rangle}{dt} = M|P\rangle, \quad (\text{S3})$$

where the matrix $M = \sum_{i=1}^L \mathcal{M}_{i,i+1}$. Here $\mathcal{M}_{i,i+1}$ is a 16×16 matrix whose elements are the transition rates between local two site configurations. In steady state $M|P\rangle = 0$. The steady state can be achieved using the following two-site flux-cancellation condition

$$\mathcal{M}_{i,i+1} \mathbf{X}_i \otimes \mathbf{X}_{i+1} = \tilde{\mathbf{X}}_i \otimes \mathbf{X}_{i+1} - \mathbf{X}_i \otimes \tilde{\mathbf{X}}_{i+1}, \quad (\text{S4})$$

where

$$\begin{aligned} \mathbf{X} &= (E, A, D_1, D_2)^T, \\ \tilde{\mathbf{X}} &= (\tilde{E}, \tilde{A}, \tilde{D}_1, \tilde{D}_2)^T, \end{aligned} \quad (\text{S5})$$

where $(\cdot)^T$ denotes the transpose of the row vector (\cdot) and $\tilde{E}, \tilde{A}, \tilde{D}_{1,2}$ are auxiliary matrices that are introduced to satisfy the steady state equation and these have to be found out consistently along with the matrix representations for $E, D, D_{1,2}$. We find that suitable choices for the auxiliary matrices are

$$\tilde{E} = 1, \quad \tilde{A} = 0, \quad \tilde{D}_1 = 0, \quad \tilde{D}_2 = 0. \quad (\text{S6})$$

The above choices of the auxiliary matrices lead us to the following matrix algebra

$$\begin{aligned} p_1 D_1 E - q_1 E D_1 &= D_1, \\ p_2 D_2 E - q_2 E D_2 &= D_2, \\ \epsilon A E &= A, \\ w_{12} D_1 A &= w_{21} D_2 A. \end{aligned} \quad (\text{S7})$$

A valid set of infinite dimensional representations of the matrices satisfying the algebra Eq. (S7), are

$$\begin{aligned}
E &= \begin{pmatrix} 0 & 0 & 0 & 0 & \dots \\ 1 & 0 & 0 & 0 & \dots \\ 0 & 1 & 0 & 0 & \dots \\ 0 & 0 & 1 & 0 & \dots \\ 0 & 0 & 0 & 1 & \dots \\ \vdots & \vdots & \vdots & \vdots & \ddots \end{pmatrix}, \quad A = \begin{pmatrix} 1 & \frac{1}{\epsilon} & \frac{1}{\epsilon^2} & \frac{1}{\epsilon^3} & \dots \\ 0 & 0 & 0 & 0 & \dots \\ 0 & 0 & 0 & 0 & \dots \\ \vdots & \vdots & \vdots & \vdots & \ddots \end{pmatrix} \\
D_I &= \begin{pmatrix} d_I^{1,1} & d_I^{1,2} & d_I^{1,3} & d_I^{1,4} & \dots \\ 0 & d_I^{2,2} & d_I^{2,3} & d_I^{2,4} & \dots \\ 0 & 0 & d_I^{3,3} & d_I^{3,4} & \dots \\ 0 & 0 & 0 & d_I^{4,4} & \dots \\ \vdots & \vdots & \vdots & \vdots & \ddots \end{pmatrix}, \quad I = 1, 2 \\
d_I^{m,m+r} &= \frac{(m)_r}{r! p_I^r} \left(\frac{q_I}{p_I} \right)^{m-1} d_I^{1,1}, \quad \forall r \geq 0 \\
d_1^{1,1} &= w_{21}, \quad d_2^{1,1} = w_{12}.
\end{aligned} \tag{S8}$$

The notation $(m)_r$ corresponds to Pochhammer symbol for rising factorials, $(m)_r := m(m-1)(m-2)\dots(m+r-1)$. For more than two species, similar kind of matrix representations do work, with the only change in the expressions for $d_I^{1,1}$ ($I = 1, 2, \dots, \mu$) [S2].

II. CALCULATION OF PARTITION FUNCTION

In this appendix, we provide the outline for calculating partition function in the steady state corresponding to the initial configuration considered in the main text. To start with, the initial configuration $C(0)$ corresponding to $\eta = 0$ is,

$$C(0) = D_2 A \dots D_2 A D_1 A \dots D_1 A D_1 \dots D_1 E \dots E. \tag{S9}$$

We note that any possible configuration C_{ss} in the steady state, starting from initial configuration Eq. (S9), would be of the following form:

$$C_{ss} = (\tau D_1 + (1-\tau)D_2)E^{m_1} A E^{\bar{m}_1} \dots (\tau D_1 + (1-\tau)D_2)E^{m_{N_+}} A E^{\bar{m}_{N_+}} D_1 E^{n_1} \dots D_1 E^{n_{\bar{N}}}, \tag{S10}$$

where τ can be either 0 or 1 and the total number of vacancies N_0 in the system, is

$$N_0 = \sum_{i=1}^{N_+} (m_i + \bar{m}_i + n_i) + \sum_{j=1}^{\bar{N}} n_j. \tag{S11}$$

For convenience, we calculate the partition function in the grand canonical ensemble by associating the fugacity z_0 with the vacancies (0). Consequently, the partition function would be

$$Q = \sum_{m_1=0}^{\infty} \dots \sum_{m_{N_+}=0}^{\infty} \sum_{\bar{m}_1=0}^{\infty} \dots \sum_{\bar{m}_{N_+}=0}^{\infty} \sum_{n_1=0}^{\infty} \dots \sum_{n_{\bar{N}}=0}^{\infty} \text{Tr} \left[\prod_{i=1}^{N_+} (D_1 + D_2)(z_0 E)^{m_i} A (z_0 E)^{\bar{m}_i} \prod_{j=1}^{\bar{N}} D_1 (z_0 E)^{n_j} \right]. \tag{S12}$$

We would use the explicit matrix representations from Eq. (S8) to calculate the partition function in Eq. (S12). It is suitable to write down the matrices in the concise form as below

$$\begin{aligned}
E &= \sum_{\gamma=1}^{\infty} |\gamma+1\rangle \langle \gamma| \Rightarrow E^n = \sum_{\gamma=1}^{\infty} |\gamma+n\rangle \langle \gamma|, \\
D_{1,2} &= \sum_{\alpha=1}^{\infty} \sum_{\beta=\alpha}^{\infty} (d_{1,2})_{\alpha,\beta} |\alpha\rangle \langle \beta|, \quad (d_{1,2})_{\alpha,\beta} := \frac{(\beta-1)!}{(\alpha-1)!(\beta-\alpha)!} \frac{q_{1,2}^{\alpha-1}}{p_{1,2}^{\beta-1}}, \\
A &= \sum_{\delta=1}^{\infty} \frac{1}{\epsilon^{\delta-1}} |1\rangle \langle \delta|,
\end{aligned} \tag{S13}$$

where $\langle k| = (0, 0, \dots, 1, \dots, 0)$ is a standard basis vector with only non-zero element 1 at the k -th place and $|k\rangle = (0, 0, \dots, 1, \dots, 0)^T$ where the superscript T denotes transpose of the vector under consideration. With the above expressions, we can simplify the matrix strings in Eq. (S12). For example, we obtain

$$\prod_{j=1}^{\bar{N}} D_1(z_0 E)^{n_j} = \sum_{n_1} \cdots \sum_{n_{\bar{N}}} \sum_{\alpha_1} \sum_{\alpha_2} \cdots \sum_{\alpha_{\bar{N}}} \sum_{\beta_{\bar{N}}} z_0^{n_1 + \cdots + n_{\bar{N}}} \times \\ (d_1)_{\alpha_1, \alpha_2 + n_1} (d_1)_{\alpha_2, \alpha_3 + n_2} (d_1)_{\alpha_3, \alpha_4 + n_3} \cdots (d_1)_{\alpha_{\bar{N}-1}, \alpha_{\bar{N}} + n_{\bar{N}-1}} (d_1)_{\alpha_{\bar{N}}, \beta_{\bar{N}} + n_{\bar{N}}} |\alpha_1\rangle \langle \beta_{\bar{N}}|. \quad (\text{S14})$$

We incorporate the explicit form of $(d_1)_{\alpha, \beta}$ from Eq. (S13) to evaluate the sums in Eq. (S14). However, it is instructive to perform the above calculation recursively, i.e. first for single D_1 , then two D_1 , followed by three D_1 and finally generalize the result for \bar{N} D_1 -s by noting the trend. On the other hand, after invoking Eq. (S13), the other string of matrices in Eq. (S12) reduces to

$$\prod_{i=1}^{N_+} (D_1 + D_2)(z_0 E)^{m_i} A(z_0 E)^{\bar{m}_i} = \left(\sum_{m_1} z_0^{m_1} \sum_{\alpha_1} ((d_1)_{\alpha_1, 1+m_1} + (d_2)_{\alpha_1, 1+m_1}) |\alpha_1\rangle \right) \times \\ \left(\sum_m \sum_n \frac{z_0^{m+n}}{\epsilon^{n-1}} \sum_{\alpha} \left(\frac{(d_1)_{\alpha, 1+m}}{\epsilon^{\alpha}} + \frac{(d_2)_{\alpha, 1+m}}{\epsilon^{\alpha}} \right) \right)^{N_+-1} \times \\ \sum_{\bar{m}_{N_+}} z_0^{\bar{m}_{N_+}} \sum_{\delta_{N_+}} \frac{\langle \delta_{N_+} |}{\epsilon^{\delta_{N_+} - 1 + \bar{m}_{N_+}}}. \quad (\text{S15})$$

Using Eqs. (S14) and (S15) in Eq. (S12), along with the explicit forms of $(d_{1,2})_{\alpha, \beta}$ from Eq. (S13), we finally arrive at the following expression of the partition function

$$Q = \left(\frac{1}{1 - \frac{z_0}{\epsilon}} \right)^{N_+} \left[\frac{w_{21}}{1 - \frac{z_0}{p_1} - \frac{z_0 q_1}{\epsilon p_1}} + \frac{w_{12}}{1 - \frac{z_0}{p_2} - \frac{z_0 q_2}{\epsilon p_2}} \right]^{N_+-1} \\ \times \prod_{k=1}^{\bar{N}} \frac{w_{21}}{1 - \frac{z_0}{p_1} S_{k-1}} \times \left[\frac{w_{21}}{1 - \frac{z_0}{p_1} S_{\bar{N}}} + \frac{w_{12}}{1 - \frac{z_0}{p_2} - \frac{q_2 z_0}{p_2 p_1} S_{\bar{N}-1}} \right], \quad (\text{S16})$$

where

$$S_k = \sum_{j=0}^k \left(\frac{q_1}{p_1} \right)^j + \left(\frac{q_1}{p_1} \right)^k \frac{q_1}{\epsilon} = \frac{p_1 \left[\left(\frac{q_1}{p_1} \right)^{k+1} ((k+1)(p_1 - q_1) - \epsilon) + \epsilon \right]}{(p_1 - q_1)\epsilon}. \quad (\text{S17})$$

Thus, we have obtained the analytical form of the partition function Eq. (S17) corresponding to the initial configuration Eq. (S9), the fugacity z_0 is computed from the density-fugacity relation

$$\rho_0 = \frac{z_0}{L} \frac{d}{dz_0} \ln Q. \quad (\text{S18})$$

Similar steps are followed to find the partition function for the more general case of non-zero η representing the initial configuration used to discuss the role of non-ergodicity on clustering, in the main text. Without going into the details, we give below the partition function corresponding to such initial configuration,

$$Q(\eta) = \left(\frac{1}{1 - \frac{z_0}{\epsilon}} \right)^{N_+} \left[\frac{w_{21}}{1 - \frac{z_0}{p_1} - \frac{z_0 q_1}{\epsilon p_1}} + \frac{w_{12}}{1 - \frac{z_0}{p_2} - \frac{z_0 q_2}{\epsilon p_2}} \right]^{N_+ - \eta \bar{N} - 1} \\ \times \left(\frac{w_{21}}{1 - \frac{z_0}{p_1} - \frac{z_0 q_1}{\epsilon p_1}} \right)^{\eta \bar{N}} \left[\frac{w_{21}}{1 - \frac{z_0}{p_1} \left(1 + \frac{q_1}{p_1} + \frac{q_1 q_1}{p_1 \epsilon} \right)} + \frac{w_{12}}{1 - \frac{z_0}{p_2} \left(1 + \frac{q_2}{p_1} + \frac{q_2 q_1}{p_1 \epsilon} \right)} \right]^{\eta \bar{N}} \\ \times \prod_{k=1}^{(1-\eta)\bar{N}} \frac{w_{21}}{1 - \frac{z_0}{p_1} S_{k-1}} \times \left[\frac{w_{21}}{1 - \frac{z_0}{p_1} S_{(1-\eta)\bar{N}}} + \frac{w_{12}}{1 - \frac{z_0}{p_2} - \frac{q_2 z_0}{p_2 p_1} S_{(1-\eta)\bar{N}-1}} \right]. \quad (\text{S19})$$

It is straightforward to check that, for $\eta = 0$ the partition function in Eq. (S19) reduces to Eq. (S17), and for the even simpler case $\bar{\rho} = 0$ it correctly reduces to the partition function considered in Ref. [S2].

III. DERIVATION OF THE OBSERVABLES

Here we sketch the steps for calculating the observables of interest, the average species densities, average drift current and n -point correlation function between consecutive vacancies. The average density ρ_1 of species 1, can be written as

$$\begin{aligned} \rho_1 = \langle 1 \rangle = \bar{\rho} + \frac{(\rho_+ - \frac{1}{L})}{Q} \sum_{m_1=0}^{\infty} \cdots \sum_{n_{\bar{N}}=0}^{\infty} \text{Tr} \left[D_1(z_0 E)^{m_1} A(z_0 E)^{\bar{m}_1} \prod_{i=2}^{N_+} (D_1 + D_2)(z_0 E)^{m_i} A(z_0 E)^{\bar{m}_i} \prod_{j=1}^{\bar{N}} D_1(z_0 E)^{n_j} \right] \\ + \frac{1}{L} \frac{1}{Q} \sum_{m_1=0}^{\infty} \cdots \sum_{n_{\bar{N}}=0}^{\infty} \text{Tr} \left[\prod_{i=1}^{N_+-1} (D_1 + D_2)(z_0 E)^{m_i} A(z_0 E)^{\bar{m}_i} D_1(z_0 E)^{m_{N_+}} A(z_0 E)^{\bar{m}_{N_+}} \prod_{j=1}^{\bar{N}} D_1(z_0 E)^{n_j} \right]. \end{aligned} \quad (\text{S20})$$

The term $\bar{\rho}$ appears directly due to the initial density $\bar{\rho}$ of the non-flipping species 1 particles. In the second part with pre-factor $(\rho_+ - \frac{1}{L})$, we place at least one D_1 in a flipping term whereas any other flipping term can have D_1 or D_2 , the density of such terms is $(\rho_+ - \frac{1}{L})$. The last part contributes due to the D_1 that is placed in the last flipping term after which the non-flipping D_1 -s start. To proceed, we would use the explicit matrix representations to evaluate the matrix strings in Eq. (S20), and we arrive at the following expression

$$\rho_1 = \bar{\rho} + \left(\rho_+ - \frac{1}{L} \right) \frac{\frac{w_{21}}{1 - \frac{z_0}{p_1} S_0}}{\left[\frac{w_{21}}{1 - \frac{z_0}{p_1} S_0} + \frac{w_{12}}{1 - \frac{z_0}{p_2} (1 + \frac{q_2}{p_1} S_{-1})} \right]} + \frac{1}{L} \frac{\frac{w_{21}}{1 - \frac{z_0}{p_1} S_{\bar{N}}}}{\left[\frac{w_{21}}{1 - \frac{z_0}{p_1} S_{\bar{N}}} + \frac{w_{12}}{1 - \frac{z_0}{p_2} (1 + \frac{q_2}{p_1} S_{\bar{N}-1})} \right]}. \quad (\text{S21})$$

Of course, the average density of species 2 would be simply $\rho_2 = \bar{\rho} + \rho_+ - \rho_1$. We can generalize this approach to calculate the average species densities for the non-zero η case. In similar manner, we obtain,

$$\begin{aligned} \rho_1(\eta) = \bar{\rho} + \left(\rho_+ - \frac{1}{L} - \eta \bar{\rho} \right) \frac{\frac{w_{21}}{1 - \frac{z_0}{p_1} S_0}}{\left[\frac{w_{21}}{1 - \frac{z_0}{p_1} S_0} + \frac{w_{12}}{1 - \frac{z_0}{p_2} (1 + \frac{q_2}{p_1} S_{-1})} \right]} + \eta \bar{\rho} \frac{\frac{w_{21}}{1 - \frac{z_0}{p_1} S_1}}{\left[\frac{w_{21}}{1 - \frac{z_0}{p_1} S_1} + \frac{w_{12}}{1 - \frac{z_0}{p_2} (1 + \frac{q_2}{p_1} S_0)} \right]} \\ + \frac{1}{L} \frac{\frac{w_{21}}{1 - \frac{z_0}{p_1} S_{(1-\eta)\bar{N}}}}{\left[\frac{w_{21}}{1 - \frac{z_0}{p_1} S_{(1-\eta)\bar{N}}} + \frac{w_{12}}{1 - \frac{z_0}{p_2} (1 + \frac{q_2}{p_1} S_{(1-\eta)\bar{N}-1})} \right]}, \\ \rho_2(\eta) = \bar{\rho} + \rho_+ - \rho_1(\eta), \end{aligned} \quad (\text{S22})$$

The drift currents for the non-conserved species and impurities are given by

$$\begin{aligned} J_{10} = p_1 \langle 10 \rangle - q_1 \langle 01 \rangle = z_0 \rho_1, \\ J_{20} = p_2 \langle 10 \rangle - q_2 \langle 01 \rangle = z_0 \rho_2, \\ J_{+0} = \epsilon \langle +0 \rangle = z_0 \rho_+. \end{aligned} \quad (\text{S23})$$

We directly replace the expressions for the non-conserved species densities from Eq. (S22) into Eq. (S23).

The formal expression for two-point nearest neighbor correlation between vacancies is

$$C_{00} = \langle 00 \rangle - \rho_0^2. \quad (\text{S24})$$

It is difficult to calculate $\langle 00 \rangle$ directly using the matrix representations, rather it is easier to use the following conservation

$$\langle 00 \rangle + \langle 01 \rangle + \langle 02 \rangle + \langle 0+ \rangle = \rho_0. \quad (\text{S25})$$

Using Eq. (S25) into Eq. (S24), we get

$$C_{00} = \rho_0 - \rho_0^2 - \langle 01 \rangle - \langle 02 \rangle - \langle 0+ \rangle. \quad (\text{S26})$$

Evaluating $\langle 01 \rangle$, $\langle 02 \rangle$ and $\langle 0+ \rangle$ using the matrix representations, we finally obtain the following expression for C_{00} as

$$C_{00} = \rho_0 - \rho_0^2 - \left(\rho_+ - \frac{1}{L} \right) \frac{z_0}{\epsilon} - \frac{1}{L} \frac{z_0}{p_1} \sum_{k=0}^{\bar{N}-1} S_k - \left(\rho_+ - \frac{1}{L} \right) \frac{\frac{w_{21} X_1}{1 - X_1} + \frac{w_{12} X_2}{1 - X_2}}{\frac{w_{21}}{1 - X_1} + \frac{w_{12}}{1 - X_2}} - \frac{1}{L} \frac{\frac{w_{21} Y_1}{1 - Y_1} + \frac{w_{12} Y_2}{1 - Y_2}}{\frac{w_{21}}{1 - Y_1} + \frac{w_{12}}{1 - Y_2}}, \quad (\text{S27})$$

where

$$\begin{aligned}
X_1 &= \frac{z_0}{p_1} + \frac{z_0 q_1}{\epsilon p_1}, \\
X_2 &= \frac{z_0}{p_2} + \frac{z_0 q_2}{\epsilon p_2}, \\
Y_1 &= \frac{z_0}{p_1} S_{\bar{N}}, \\
Y_2 &= \frac{z_0}{p_2} + \frac{z_0 q_2}{p_1 p_2} S_{\bar{N}-1}.
\end{aligned} \tag{S28}$$

Clearly, the two-point correlation would have a closed form if the sum $\sum_{k=0}^{\bar{N}-1} S_k$ has a closed form, and indeed this can be evaluated as

$$\begin{aligned}
\frac{1}{L} \sum_{k=0}^{\bar{N}-1} S_k &= \frac{\bar{N}}{L} \frac{p_1}{(p_1 - q_1)} + \frac{1}{L} \left[1 - \left(\frac{q_1}{p_1} \right)^{\bar{N}} \right] \left(\frac{p_1 - q_1}{\epsilon} - 1 \right) \frac{p_1 q_1}{(p_1 - q_1)^2} \\
&= \bar{\rho} \frac{p_1}{(p_1 - q_1)} + \frac{1}{L} \left[1 - \left(\frac{q_1}{p_1} \right)^{\bar{N}} \right] \left(\frac{p_1 - q_1}{\epsilon} - 1 \right) \frac{p_1 q_1}{(p_1 - q_1)^2}
\end{aligned} \tag{S29}$$

So, we have evaluated the two-point correlation function C_{00} exactly. Of course, z_0 has to be calculated from the density-fugacity relation. Importantly in Eq. (S29), note that we could scale \bar{N} by system-size L properly in the first term so that it becomes a function of $\bar{\rho}$, but this is not possible in case of the second term where \bar{N} appears in the power.

In fact, using the result of C_{00} , we can calculate C_{000} and then C_{0000} using C_{000} , and so on. For simplified notations, we denote $C_0^{[n]}$ as the correlation between consecutive n vacancies, then we obtain in iterative way,

$$\begin{aligned}
C_0^{[2]} &= \rho_0 - \rho_0^2 - \left(\rho_+ - \frac{1}{L} \right) \frac{z_0}{\epsilon} - \frac{1}{L} \frac{z_0}{p_1} \sum_{k=0}^{\bar{N}-1} S_k \\
&\quad - \left(\rho_+ - \frac{1}{L} \right) \frac{\frac{w_{21} X_1}{1-X_1} + \frac{w_{12} X_2}{1-X_2}}{\frac{w_{21}}{1-X_1} + \frac{w_{12}}{1-X_2}} - \frac{1}{L} \frac{\frac{w_{21} Y_1}{1-Y_1} + \frac{w_{12} Y_2}{1-Y_2}}{\frac{w_{21}}{1-Y_1} + \frac{w_{12}}{1-Y_2}}, \\
C_0^{[3]} &= C_0^{[2]} + \rho_0^2 - \rho_0^3 - \left(\rho_+ - \frac{1}{L} \right) \left(\frac{z_0}{\epsilon} \right)^2 - \frac{1}{L} \left(\frac{z_0}{p_1} \right)^2 \sum_{k=0}^{\bar{N}-1} (S_k)^2 \\
&\quad - \left(\rho_+ - \frac{1}{L} \right) \frac{\frac{w_{21} X_1^2}{1-X_1} + \frac{w_{12} X_2^2}{1-X_2}}{\frac{w_{21}}{1-X_1} + \frac{w_{12}}{1-X_2}} - \frac{1}{L} \frac{\frac{w_{21} Y_1^2}{1-Y_1} + \frac{w_{12} Y_2^2}{1-Y_2}}{\frac{w_{21}}{1-Y_1} + \frac{w_{12}}{1-Y_2}}, \\
C_0^{[4]} &= C_0^{[3]} + \rho_0^3 - \rho_0^4 - \left(\rho_+ - \frac{1}{L} \right) \left(\frac{z_0}{\epsilon} \right)^3 - \frac{1}{L} \left(\frac{z_0}{p_1} \right)^3 \sum_{k=0}^{\bar{N}-1} (S_k)^3 \\
&\quad - \left(\rho_+ - \frac{1}{L} \right) \frac{\frac{w_{21} X_1^3}{1-X_1} + \frac{w_{12} X_2^3}{1-X_2}}{\frac{w_{21}}{1-X_1} + \frac{w_{12}}{1-X_2}} - \frac{1}{L} \frac{\frac{w_{21} Y_1^3}{1-Y_1} + \frac{w_{12} Y_2^3}{1-Y_2}}{\frac{w_{21}}{1-Y_1} + \frac{w_{12}}{1-Y_2}}, \\
&\quad \dots = \dots \\
C_0^{[n]} &= C_0^{[n-1]} + \rho_0^{n-1} - \rho_0^n - \left(\rho_+ - \frac{1}{L} \right) \left(\frac{z_0}{\epsilon} \right)^{n-1} - \frac{1}{L} \left(\frac{z_0}{p_1} \right)^{n-1} \sum_{k=0}^{\bar{N}-1} (S_k)^{n-1} \\
&\quad - \left(\rho_+ - \frac{1}{L} \right) \frac{\frac{w_{21} X_1^{n-1}}{1-X_1} + \frac{w_{12} X_2^{n-1}}{1-X_2}}{\frac{w_{21}}{1-X_1} + \frac{w_{12}}{1-X_2}} - \frac{1}{L} \frac{\frac{w_{21} Y_1^{n-1}}{1-Y_1} + \frac{w_{12} Y_2^{n-1}}{1-Y_2}}{\frac{w_{21}}{1-Y_1} + \frac{w_{12}}{1-Y_2}}.
\end{aligned} \tag{S30}$$

Thus we have obtained the analytical formulae for average species densities, drift currents and n -point correlation between consecutive vacancies.

IV. DENSITY-FUGACITY RELATION: SOLUTION FOR SPECIAL CASES

Here we would like to state the explicit form of the density-fugacity relation, calculated from the partition function in Eq. (S16). This relation is used to solve the fugacity z_0 as a function of the input parameters. Consequently, we

can replace the corresponding value of z_0 in the expressions of the observables e.g. in Eqs. (S21), (S23) and (S27) so that they become functions of the input parameters only. The formal expression for the density-fugacity relation is

$$\rho_0 = \frac{z_0}{L} \frac{d}{dz_0} \ln Q, \quad (\text{S31})$$

where the partition function Q is given by Eq. (S16) corresponding to the initial configuration considered in the main text. Therefore, we have the following density-fugacity relation to solve,

$$\begin{aligned} & \frac{z_0 \left(\rho_+ - \frac{1}{L}\right)}{w_{21}(1 - z_0 X'_2) + w_{12}(1 - z_0 X'_1)} \left[w_{21} X'_1 \frac{1 - z_0 X'_2}{1 - z_0 X'_1} + w_{12} X'_2 \frac{1 - z_0 X'_1}{1 - z_0 X'_2} \right] \\ & + \frac{\frac{z_0}{L}}{w_{21}(1 - z_0 Y'_2) + w_{12}(1 - z_0 Y'_1)} \left[w_{21} Y'_1 \frac{1 - z_0 Y'_2}{1 - z_0 Y'_1} + w_{12} Y'_2 \frac{1 - z_0 Y'_1}{1 - z_0 Y'_2} \right] \\ & + \frac{\rho_+}{1 - \frac{z_0}{\epsilon}} + \frac{1}{L} \sum_{k=1}^{\bar{N}} \frac{1}{1 - \frac{z_0}{\rho_1} S_{k-1}} = \rho_0 + \rho_+ + \bar{\rho}, \end{aligned} \quad (\text{S32})$$

with $X'_{1,2} = X_{1,2}/z_0$ and $Y'_{1,2} = Y_{1,2}/z_0$, where $X_{1,2}$ and $Y_{1,2}$ follow Eq. (S28), S_k is given by Eq. (S17). The reason behind such rescaling by z_0 , is simply to express $X'_{1,2}$ and $Y'_{1,2}$ as functions of the input parameters only. In general, we have solved Eq. (S32) in Mathematica to get z_0 for a given set of input parameters. Also note that the complexity of the equation increases with increasing number of non-flipping species 1 particles \bar{N} , in terms of the highest degree of z present in the polynomial of z_0 in Eq. (S32). For some special cases with specific choices of the hop-rates, one can obtain closed form solutions for the fugacity z_0 .

A particularly simple case corresponds to $\bar{N} = 0$. This also implies $Y'_1 = X'_1$ and $Y'_2 = X'_2$, which can be seen directly from Eq. (S28) with the help of Eq. (S17). We further consider the special situation of $X'_1 = X'_2$. The density-fugacity relation Eq. (S32) simplifies to

$$\frac{z_0 \rho_+ X'_1}{1 - z_0 X'_1} + \frac{\rho_+}{1 - \frac{z_0}{\epsilon}} = \rho_0 + \rho_+. \quad (\text{S33})$$

The above equation has the following solution

$$z_0 = \frac{(\rho_0 + \rho_+)(1 + \epsilon X'_1) + \sqrt{(\rho_0 + \rho_+)^2(1 + \epsilon X'_1)^2 - 4\rho_0 \epsilon X'_1(\rho_0 + 2\rho_+)}}{2(\rho_0 + 2\rho_+)X'_1}. \quad (\text{S34})$$

To better understand the constraint on the hop rates for which we have got the exact solution Eq. (S34), we explore the situation $X'_1 = X'_2$, which basically boils down to

$$\epsilon = \frac{q_2 p_1 - q_1 p_2}{p_2 - p_1}. \quad (\text{S35})$$

The above subspace of hop rates can create both natural flow and counter-flow situations and also includes the very special case $p_1 = p_2$ and $q_1 = q_2$. We should mention that, even without the assumption $X'_1 = X'_2$, we have a quartic equation in z_0 that can be solved exactly in Mathematica. However, the solution of z_0 in that case is too lengthy to include here.

Another noteworthy point is, the fugacity z_0 actually equals to the cluster velocity v_{c1} discussed in the main text (see inset of Fig. 3). This is evident from the current-density relation Eq. (S23), which can be considered as $J = v_{c1} \rho$ in the clustering phase. In fact, one can check the inset of Fig. 3 in the main text, obtained from Monte Carlo simulations, can be reproduced by calculating z_0 for the corresponding set of input parameters.

V. A COMMENT REGARDING THE INITIAL CONFIGURATION

We have considered step-like initial configuration in the main text. To elaborate, initially all the particles (both species and impurities) occupy consecutive lattice sites with no vacancy between them. Starting from such step-like initial configuration, in the free flowing phase, the vacancies get randomly distributed between the particles. On the other hand, in the clustering phase, any steady state configuration remains step-like, with the particle cluster shifting slowly to right. Naturally, the question arises if the cluster can be formed from an initial configuration which is not step-like, rather there are vacancies distributed between particles. The answer is *yes*. If we start from a non-step-like initial configuration given below,

$$C(0) = D_2 E^{m_1} A E^{\bar{m}_1} \dots D_2 E^{m_{N+1/2}} A E^{\bar{m}_{N+1/2}} D_1 E^{n_1} A E^{\bar{n}_1} \dots D_1 E^{n_{N+1/2}} A E^{\bar{n}_{N+1/2}} D_1 E^{r_1} \dots D_1 E^{r_{\bar{N}}}, \quad (\text{S36})$$

where the total number of vacancies is

$$\sum_{i=1}^{N_+/2} (m_i + \bar{m}_i + n_i + \bar{n}_i) + \sum_{j=1}^{\bar{N}} r_k = N_0. \quad (\text{S37})$$

Note that, the above initial configuration contains exact same ordering of particles just like the one studied in the

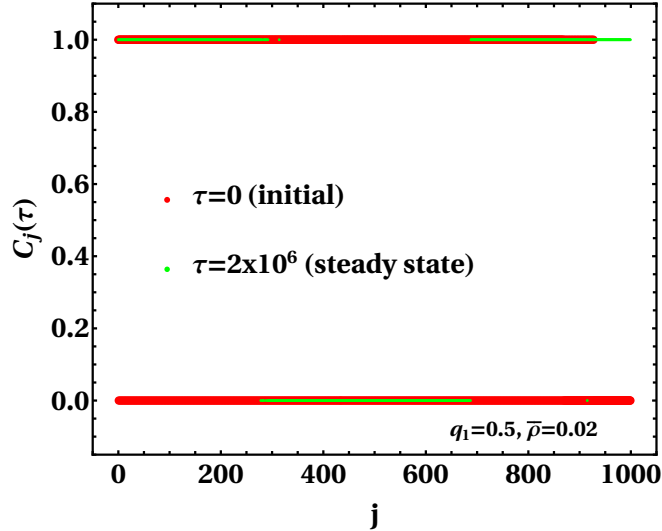
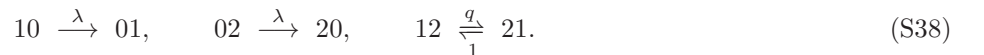


FIG. S1. The figure demonstrates the step-like cluster (green dots) formation in the steady state, starting from a non-step-like initial configuration (red dots) where vacancies are randomly distributed among particles. The parameters used are $L = 10^3$, $p_1 = 0.4$, $p_2 = 1.0$, $q_2 = 0.5$, $\epsilon = 0.1$, $w_{12} = 1.0$, $w_{21} = 0.1$, $\rho_+ = 0.29$, $\rho_0 = 0.4$. The counter-flow situation is ensured by the choice $q_1 (= 0.5) > p_1 (= 0.4)$.

main text and the total number of vacancies are also the same for both configurations, only difference being the initial configuration in the main text is step-like, whereas Eq. (S36) is non-step-like. Since the ordering of vacancies actually do not matter, both of these initial configurations lead to the same configuration sub-space in the steady state. Thereby all the characteristics of the system in the steady state remain same for both of these initial configurations. Thus we expect to see the clustering phenomena starting from initial configuration Eq. (S36) just like we did for the one in the main text. Indeed, in Fig. S1, we observe that the macroscopic cluster is formed in the steady state, while the initial configuration is non-step-like. So, the only advantageous and satisfactory thing about Eq. (S36), is the fact that the cluster is formed in a dynamic way from non-step-like initial configuration.

VI. ARNDT-HEINZEL-RITTENBERG MODEL OF COUNTER-FLOW: COMPARISONS

In this section, we compare the microscopic dynamics of our model with the dynamics of the Arndt-Heinzl-Rittenberg (AHR) model that is known to exhibit three different phases [S1, S3, S4]. The AHR model considers positive (say, species 1) and negative (say, species 2) particles along with vacancies (0) on a one dimensional periodic lattice and the follow the dynamical rules given below



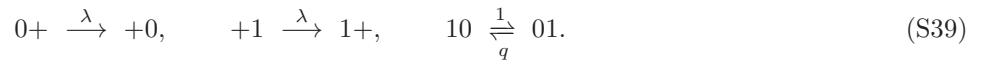
A straightforward comparison of the AHR model in Eq. (S38) with our model in Eq. (S1) reveal the following factors: (i) our model allows a *non-conserving flip dynamics* that activates transformations between species 1 and 2, which is absent in the AHR model for which each microscopic dynamics maintains particle number conservation of every species. Also, as a consequence, our model requires minimum four species in total (species 1, species 2, impurity and vacancy) to operate both drift and flip dynamics, while the AHR model deals with three species in total (species 1, species 2, and vacancy). (ii) AHR model has an *exchange dynamics* that allows the two species to exchange their positions. Such exchange dynamics is absent in our case. (iii) Our model is *non-ergodic* in contrast to the *ergodic* nature of the AHR model.

The exchange rate q is considered as the tuning parameter for the AHR model and the density ρ of the two species are taken to be equal [S1, S4]. Three different phases, namely *pure phase*, *mixed phase* and *disordered phase* are observed, as q is varied [S1, S4]. When $q < 1$, the species 1 is more probable to reside at left of species 2 which again likes to be at left of vacancies. This leads to a complete species segregation with three types of blocks each purely consisting of one species (either 1 or 2 or 0), thereby referred as pure phase. For $1 < q < q_c$ (where q_c depends on λ and ρ), a condensate is formed that has both species 1 and species 2 mixed up, accompanied by a fluid consisting of vacancies and some particles of the two species. This phase is known as the mixed phase. There is no species segregation or condensate formation for $q > q_c$, which is the disordered phase. To observe these three phases, two point functions like drift current and correlations between different species, have been used [S1, S4].

Interestingly, in our model, due to the presence of non-conserving flip dynamics, we have even simpler one point function like average species densities among observables of interest, and indeed the average species densities clearly show the existence of two different phase, the *free flowing phase* and the *clustering phase*. The free flowing phase in our model is similar to the disordered phase of AHR model. On the other hand, for the specific choice of initial configuration considered here and due to the flip dynamics, species segregation in *pure* form is not possible in the clustering phase. Rather, we have two macroscopic clusters, one consisting of only vacancies and the other consisting of all kinds of particles (species 1 and species 2 and impurities). Although the mixing up of different species and impurities inside the particle cluster has resemblance to the mixed phase condensate of AHR model, we do not have a background fluid in our case. Rather, for any $q_1 > p_1$, we have only two clusters in the clustering phase, a vacancy cluster and a particle cluster, with the particle cluster drifting along right with considerably small velocity that depends on the density of the non-flipping species 1 particles in the system. Another noteworthy point in our analysis is the *rearrangement parameter* whose variation captures the effect of non-ergodicity on the clustering phenomenon, there is no such counterpart in the ergodic AHR model.

Note that exact analysis in Refs. [S5] and [S6] later revealed that there is actually no phase transition between mixed and disordered phase in the AHR model, in the thermodynamic limit within the grand canonical ensemble framework. This conclusion is associated with the existence of extremely long but still finite correlation lengths in the infinite system.

There is an alternative approach to compare the dynamics of the two models, although the key points of the comparative analysis between them remain the same. Our tuning parameter has been the counter-flow parameter q_1 , which is a part of the drift dynamics. To treat the tuning parameter q of the AHR model on an equivalent footing, one can relabel species 1, species 2 and vacancy in AHR model as vacancy, species 1 and species + respectively. Thus one arrives at an alternative version of the AHR model given below



Here we see, in comparison to our model Eq. (S1), the species 2 is absent and we do not term + as impurity because there is no flip dynamics at all. So + drifts to left only, species 1 drifts to right or left with rates q and 1 respectively, with an additional exchange of positions between + and 1. Clearly $q > 1$ here corresponds to natural flow situation and $q < 1$ refers to the counter-flow situation.

The exact steady state of AHR model in Eq. (S38) has been obtained in matrix product form, which has a two dimensional representation in the limit $q \rightarrow \infty$ and infinite dimensional representations in general [S4], which have different structures in comparison to the infinite dimensional matrices in our case Eq. (S8).

[S1] P. F. Arndt, T. Heinzl, and V. Rittenberg, J. Phys. A: Math. Gen. **31**, L45 (1998), doi:10.1088/0305-4470/31/2/001.

[S2] A. K. Chatterjee, and H. Hayakawa, [arXiv:2205.03082](https://arxiv.org/abs/2205.03082) (2022).

[S3] P. F. Arndt, T. Heinzl, and V. Rittenberg, J. Phys. A: Math. Gen. **31**, 833 (1998), doi:10.1088/0305-4470/31/3/003.

[S4] P. F. Arndt, T. Heinzl, and V. Rittenberg, J. Stat. Phys. **97**, 1 (1999), doi:10.1023/A:1004670916674.

[S5] N. Rajewsky, T. Sasamoto, and E. R. Speer, Physica A **279**, 123 (2000), doi:10.1016/S0378-4371(99)00537-3.

[S6] T. Sasamoto, and D. Zagier, J. Phys. A: Math. Gen. **34**, 5033 (2001), doi:10.1088/0305-4470/34/24/302.